

## Formulation and Numerical Solution of a Set of Dynamical Equations for the Regge Pole Parameters\*

HUNG CHENG AND DAVID SHARP†  
*California Institute of Technology, Pasadena, California*

(Received 8 July 1963)

In a previous paper, the principles of analyticity and unitarity were shown to lead to a set of coupled nonlinear integral equations for the Regge pole parameters. In this paper, we demonstrate, for both boson and fermion trajectories, that these equations can be written in a very simple form which makes many of their mathematical properties transparent and permits their numerical solution by iteration. We then proceed to carry out their numerical solution in a number of interesting cases. Because our equations are approximate, we first solved the equations in the potential-theory case, where our results could be compared with those obtained from the Schrödinger equation. The agreement in most cases is good. Then we turn to the determination of the Regge pole parameters which describe relativistic  $\pi\pi$  scattering at high energies. Neglecting the inelastic contributions, we calculate the Pomeranchuk trajectory, the  $\rho$ -meson trajectory, and the second vacuum trajectory  $P'$ . One notable result of this set of calculations is that the function  $\text{Re } \alpha(t)$  for the Pomeranchuk trajectory, as determined by our equations, agrees well with the results obtained by Foley *et al.* from an analysis of the  $\pi^-p$  angular distributions in the range  $-0.8(\text{BeV}/c)^2 < t < -0.2(\text{BeV}/c)^2$ . No spin-2 resonance is found to lie on this trajectory. As for the  $\rho$  trajectory, we find that  $\alpha_\rho(t)$ ,  $-0.8(\text{BeV}/c)^2 < t \leq 0$ , is larger than 0.9 for a wide range of input parameters. The width of the  $\rho$  resonance, as determined from our equation, is several times larger than the experimental width. This probably means that inelastic contributions must be included to obtain a correct value for the width. Finally, we outline various problems which remain to be investigated.

### I. INTRODUCTION

IF Regge poles are to play an important role in understanding the properties of high-energy scattering cross sections and of the many newly observed resonances, it appears essential to have a method for the dynamical determination of the Regge pole parameters. This belief is based on the following considerations:

(1) Recent measurements of the angular distributions in  $\pi p$  and  $pp$  scattering<sup>1-3</sup> at high energies ( $15 < s/2m_N^2 < 25$ ) have been analyzed on the basis of a Regge pole model. The constancy of the total cross sections in the two systems at these energies at first suggested that one can assume that the dominant contribution to the cross sections comes from the Pomeranchuk trajectory. That this assumption cannot be correct in both cases, at least as far as the differential cross sections are concerned, is shown by the facts that almost no diffraction shrinking is observed in the  $\pi p$  system while considerable shrinking is observed in the  $pp$  system. If the hypothesis that Regge poles dominate the high-energy scattering is still valid, it must mean that in the present energy range the analysis of the cross sections is complicated by the presence of several trajectories contributing in an important way. If this is the case, it would seem

that reasonably clear cut experimental tests of the Regge predictions about total cross sections and diffraction peaks would be possible only if the Regge pole parameters involved were known functions.

(2) There is some reason to believe<sup>4</sup> that when multi-particle states are included in the analysis of relativistic scattering processes, the analyticity properties of the  $S$  matrix in the  $J$  plane will be complicated by the presence of cuts in addition to simple poles. This circumstance would result in further ambiguities in the interpretation of experimental data, which would be somewhat alleviated if the pole parameters were known.

(3) It is a consequence of the Regge formalism that a set of resonances or bound states, all having the same quantum numbers including  $J$  parity, but having different values of  $J$  and occurring at different energies, will all lie along the same Regge trajectory<sup>5,6</sup>  $\alpha(t)$ . The existence of Regge cuts should not lead to any ambiguities in experimentally establishing the existence and properties of any such resonances. For this reason, the possibility of grouping the new resonances in Regge families, and of correlating a set of resonance parameters with each other and with the observed total cross sections and angular distributions remains as an interesting application of the Regge theory. To make good use of this possibility, however, it seems essential to have a method with which to determine the Regge pole parameters.

In a previous paper,<sup>7</sup> the authors made use of the

\* Work supported in part by the U. S. Atomic Energy Commission. Part of the work reported here is included in a thesis to be submitted by David H. Sharp to the California Institute of Technology in partial fulfillment of the requirements for the degree of Doctor of Philosophy.

† National Science Foundation Predoctoral Fellow, 1960-63.

<sup>1</sup> K. J. Foley, S. J. Lindenbaum, W. A. Love, S. Ozaki, J. J. Russell, and L. C. L. Yuan, *Phys. Rev. Letters* **10**, 376 (1963).

<sup>2</sup> C. C. Ting, L. W. Jones, and M. L. Perl, *Phys. Rev. Letters* **9**, 468 (1962).

<sup>3</sup> A. N. Diddens, E. Lillethun, G. Manning, A. E. Taylor, T. G. Walker, and A. M. Wetherell, *Phys. Rev. Letters* **9**, 108, 111 (1962).

<sup>4</sup> S. Mandelstam, lecture given at the California Institute of Technology, January 1963, and private communication.

<sup>5</sup> R. Blankenbecler and M. L. Goldberger, *Phys. Rev.* **126**, 766 (1962).

<sup>6</sup> G. F. Chew and S. C. Frautschi, *Phys. Rev. Letters* **8**, 41 (1962).

<sup>7</sup> H. Cheng and D. Sharp, *Ann. Phys. (N. Y.)* **22**, 481 (1963).

analytic properties of the Regge pole parameters  $\alpha(t)$  and  $r(t)$  plus the unitarity condition satisfied by the partial-wave amplitude to derive a coupled set of integral equations which determine the location  $\alpha(t)$  and the residue  $r(t)$  of a Regge pole as functions of  $t$ . The equations obtained are approximate in that: (i) Only two-body scattering processes are included, and (ii) the unitarity condition is employed in a form which is valid only when  $\text{Im}\alpha(t)$  is small. This latter condition implies that the influence of the coupling of one Regge pole to another is neglected. Many aspects of these equations were not understood at the time, in particular, the circumstances under which a unique solution might exist were not known. Moreover, numerical solutions had not been obtained and a quantitative idea of the usefulness or range of validity of the approximations made had not been arrived at.

It is our purpose in this paper to discuss the properties of the above mentioned equations in considerably more detail and to obtain numerical solutions of them in several interesting cases.

In Sec. II, we show how to transform our original set of equations so as to obtain an integral equation involving the *single* unknown function  $\text{Im}\alpha(t)$ . Once  $\text{Im}\alpha(t)$  is obtained by solving this equation, we obtain  $\text{Re}\alpha(t)$  and the residue  $r(t)$  by performing simple integral transforms. The derivation has been carried out for boson and fermion Regge trajectories.

Because the equations we use are approximate, it is very desirable to compare our results for the Regge parameters with those obtained in some rigorous way. This is possible only in potential theory. Consequently, in Sec. III, we specialize the equations derived in Sec. II to their nonrelativistic form. We also make in Sec. III a number of comments on the more formal mathematical properties of these equations, especially those related to the uniqueness question.

In Sec. IV, we present our calculations of the Regge parameters in the case of scattering in a single Yukawa potential of unit range. A wide variety of potential strengths are considered. These results are critically compared to those obtained by Ahmadzadeh, Burke, and Tate<sup>8</sup> and by Lovelace and Masson.<sup>9</sup>

In Sec. V, we solve the equations for the case of relativistic  $\pi\pi$  scattering. In the case of  $\pi\pi$  scattering, we have obtained the positions of the poles describing the Pomeranchuk trajectory, the  $\rho$ -meson trajectory, and the second vacuum trajectory introduced by Igi.<sup>10</sup> The properties of the  $P$  trajectory, as computed from our equations, agree well with those ascertained by Foley *et al.*<sup>1</sup> from an analysis of  $\pi^-p$  angular distributions. We use our results on the  $\rho$ -meson trajectory to obtain  $\alpha_\rho(t)$ ,  $t \leq 0$ , which governs the energy

dependence of  $\sigma_{\pi^-p} - \sigma_{\pi^+p}$  and of the corresponding angular distributions.

Finally, in Sec. VI, we summarize the conclusions reached in this paper and outline a number of interesting problems which remain to be investigated.

II. FORMULATION OF A SET OF INTEGRAL EQUATIONS FOR THE REGGE POLE PARAMETERS: RELATIVISTIC CASE

Let us consider the relativistic scattering of two spinless particles  $a$  and  $b$  with masses  $m_a$  and  $m_b$ . We shall discuss the Regge poles of the partial-wave amplitude in the  $t$  channel for the reaction  $a+b \rightarrow a+b$ . Our purpose in this section is to derive a set of equations which will allow an approximate dynamical determination of the position  $\alpha(t)$  of the Regge pole and of its residue  $r(t)$ , which is equal to  $\text{Res}[A(\alpha(t), t)]$ .

The authors have recently suggested<sup>7</sup> that the Regge parameters can be determined from the principles of analyticity and unitarity. If crossing<sup>11</sup> of trajectories is neglected, then both  $\alpha(t)$  and  $r(t)/q^{2\alpha(t)}$  are real analytic functions of  $t$  with branch cuts from  $T_0$  to  $\infty$ , where  $T_0$  is the threshold value of  $t$  for the reaction  $a+b \rightarrow a+b$ .

The function  $\alpha(t)$  is assumed to have a behavior at infinity which permits us to express its real analyticity by means of a dispersion relation of the simple form

$$\alpha(t) = \alpha_0 + \frac{t - t_0}{\pi} \int_{T_0}^{\infty} \frac{\text{Im}\alpha(t') dt'}{(t' - t)(t' - t_0)}. \quad (2.1)$$

The situation is not so simple for the function  $r(t)/q^{2\alpha(t)}$ . The difficulty is that, because  $\alpha(t)$  presumably approaches a negative quantity as  $t \rightarrow \pm\infty$ , we cannot always write a dispersion relation for  $r(t)/q^{2\alpha(t)}$  in the once-subtracted form of Eq. (2.1). We can avoid this difficulty in the case of equal mass scattering by dealing with the function  $r(t)e^{-i\pi\alpha(t)}$ . But if we consider the scattering of particles of unequal mass, a dispersion relation for  $r(t)$  would be complicated by the presence of kinematic cuts coming from the factor  $q^{2\alpha(t)}$ .

We have found that, for the purpose of obtaining equations for the Regge pole parameters from the principles of analyticity and unitarity, it is wholly adequate simply to know that  $r(t)/q^{2\alpha(t)}$  is real analytic, and no occasion will arise where it is necessary to have a dispersion relation for  $r(t)/q^{2\alpha(t)}$ . Therefore, we can avoid the complications mentioned above.

We shall use the following kinematic variables:

$$\begin{aligned} t &= 4\omega^2 \\ &= \text{total c.m. energy squared in } t \text{ channel} \\ &= m_a^2 + m_b^2 + 2\{(m_a^2 + q^2)(m_b^2 + q^2)\}^{1/2} + q^2; \end{aligned} \quad (2.2a)$$

and

$$q^2 = \{[t - (m_a + m_b)^2][t - (m_a - m_b)^2]\} / 4t, \quad (2.2b)$$

<sup>8</sup> A. Ahmadzadeh, P. Burke, and C. Tate, Phys. Rev. **131**, 1315 (1963).

<sup>9</sup> C. Lovelace and D. Masson, Nuovo Cimento **26**, 472 (1962).

<sup>10</sup> K. Igi, Phys. Rev. Letters **9**, 76 (1962).

<sup>11</sup> H. Cheng, Phys. Rev. **130**, 1283 (1963).

where  $q$ =c.m. momentum of an incoming or outgoing particle.

The unitarity condition shall be written as

$$r(t) = \text{Im}\alpha(t)(\omega/q), \quad t > T_0. \quad (2.3)$$

Equation (2.3) is an approximate form of the unitarity condition

$$[A(l,t) - A^*(l^*,t)]/2i = (q/\omega)A^*(l^*,t)A(l,t) \quad (2.4)$$

which is valid when  $l \approx \alpha(t)$  and  $\text{Re}\alpha(T_0) > -\frac{1}{2}$ .

F. Zachariasen<sup>12</sup> has pointed out to us that we can use Eq. (2.1), (2.3), and the real analyticity of  $r(t)/q^{2\alpha(t)}$  to derive a very simple integral equation for  $\text{Im}\alpha(t)$ . This can be done as follows:

Since we know that the function  $r(t)/q^{2\alpha(t)}$  is real analytic, we have

$$r^*(t) = r(t^*)e^{-2i\pi\alpha(t^*)}, \quad t > T_0. \quad (2.5a)$$

According to Eq. (2.3),  $r(t^+)$  is real. Therefore,

$$r(t^+) = r(t^-)e^{-2i\pi\alpha(t^-)}, \quad t > T_0 \quad (2.5b)$$

where  $t^\pm = t \pm i\epsilon$ . Let us write

$$r(t)/(q^{2\alpha(t)}) = F(t)e^{U(t)}, \quad (2.6)$$

where  $F(t)$  is a rational function of  $t$ , and  $U(t)$  is an analytic function of  $t$  cut from  $T_0$  to  $\infty$ . The discontinuity of  $U(t)$  across the branch cut can be obtained from (2.5) and (2.6);

$$U(t^+) - U(t^-) = -2i \text{Im}\alpha(t) \ln q^2. \quad (2.7)$$

Consequently, we can apply Cauchy's theorem to the analytic function  $U(t)$  to find

$$U(t) = -\frac{(t-t_0)}{\pi} \int_{T_0}^{\infty} \frac{\ln(q'^2/q^2) \text{Im}\alpha(t')}{(t'-t)(t'-t_0)} dt', \quad (2.8)$$

where we have normalized  $U(t)$  so that  $U(t_0) = 0$ . Equations (2.1), (2.6), and (2.8) give

$$r(t) = F(t)q^{2\alpha_0} \times \exp\left\{-\frac{(t-t_0)}{\pi} \int_{T_0}^{\infty} \frac{\ln(q'^2/q^2) \text{Im}\alpha(t')}{(t'-t)(t'-t_0)} dt'\right\}, \quad (2.9)$$

where the dispersion relation for  $\alpha(t)$ , Eq. (2.1), has been used to replace  $\alpha(t)$  in (2.6) by the right side of (2.1). Equations (2.3) and (2.9) then give

$$\begin{aligned} \text{Im}\alpha(t) &= \frac{q}{\omega} F(t)q^{2\alpha_0} \\ &\times \exp\left\{-\frac{t-t_0}{\pi} \int_{T_0}^{\infty} \frac{\ln(q'^2/q^2) \text{Im}\alpha(t')}{t'-t} \frac{dt'}{t'-t_0}\right\}, \\ & \quad t > T_0. \quad (2.10) \end{aligned}$$

<sup>12</sup> F. Zachariasen (private communication). Professor Zachariasen's observation has proven to be of decisive importance in extracting useful information from our equations.

One point is worth noticing. We know that  $\text{Im}\alpha(t)$  is always real, but  $\alpha_0$  may be complex, and at first sight, the right side of (2.10) may appear to be complex. However, we can easily see that we can replace  $\alpha_0$  by  $\text{Re}\alpha_0$  and the integral by its Cauchy principle part, and then the right side of (2.10) is actually real.

Now let us determine the function  $F(t)$ . We shall assume that  $r(t)$  has no poles, in which case  $F(t)$  is entire in  $t$ . We obtain from Eq. (2.10) that

$$\begin{aligned} \text{Im}\alpha(t) &\xrightarrow{t \rightarrow \infty} \lambda F(t)q^{2\alpha_0} \exp\left\{-\frac{\ln q^2}{\pi} \int_{T_0}^{\infty} \frac{\text{Im}\alpha(t')}{t'-t_0} dt'\right\} \\ &= \lambda F(t)q^{2\alpha(\infty)}, \quad (2.11) \end{aligned}$$

where  $\lambda$  is a constant. If we now require that  $\text{Im}\alpha(t)$  vanishes as  $t \rightarrow \infty$ , then  $F(t)$ , being entire, is a polynomial of order  $n$  satisfying the inequality

$$n < -\alpha(\infty). \quad (2.12)$$

Moreover, from (2.9), we find

$$q_0^{2\alpha_0} F(t_0) = r(t_0). \quad (2.13)$$

Thus, we can infer that the general form of  $F(t)$  is

$$F(t) = \frac{r(t_0)}{q_0^{2\alpha_0}} \prod_{i=1}^n \left(\frac{t-t_i}{t_0-t_i}\right), \quad (2.14)$$

where the  $t_i$  specify the location of the zeroes of  $r(t)$ . We shall go into the question of zeroes, and the connection between the number of zeroes and the asymptotic behavior of  $\text{Im}\alpha(t)$  more fully in Sec. III which treats the potential theory case. If we suppose that the trajectory of interest has 0 or 1 zero, for example, then the resultant equations take the form:

$$\begin{aligned} \text{Im}\alpha(t) &= \frac{q}{\omega} r(t_0) 1 \left(\frac{q}{q_0}\right)^{2\alpha_0} \\ &\times \exp\left\{-\frac{t-t_0}{\pi} \int_{T_0}^{\infty} \frac{\ln(q'^2/q^2) \text{Im}\alpha(t')}{t'-t} \frac{dt'}{t'-t_0}\right\} \quad (2.15) \end{aligned}$$

or

$$\begin{aligned} &= \frac{q}{\omega} r(t_0) \left(\frac{t-t_1}{t_0-t_1}\right) \left(\frac{q}{q_0}\right)^{2\alpha_0} \\ &\times \exp\left\{-\frac{t-t_0}{\pi} \int_{T_0}^{\infty} \frac{\ln(q'^2/q^2) \text{Im}\alpha(t')}{t'-t} \frac{dt'}{t'-t_0}\right\}, \\ & \quad t > T_0. \quad (2.16) \end{aligned}$$

Equations (2.15) and (2.16) are the desired results. What we have achieved is a decoupling of Eqs. (2.1) and (2.3) so as to obtain an integral equation involving the single unknown function  $\text{Im}\alpha(t)$ . Once we have solved for  $\text{Im}\alpha(t)$ , we can obtain  $\text{Re}\alpha(t)$  by performing a simple Hilbert transform. For  $t > T_0$ ,  $r(t)$  is obtained algebraically from the unitarity condition (2.3) and,

for other values of  $l$ , it can be obtained from the dispersion relation for  $r(t)e^{-i\pi\alpha(t)}$  if  $m_a=m_b$ , and from Eq. (2.9) in the general case.

Equation (2.15) has many attractive features. It incorporates the known threshold behavior of  $\text{Im}\alpha(t)$ , it exhibits the possible zeroes of  $r(t)$  explicitly, it has a reasonable asymptotic behavior, and it is in a form which suggests the possibility of a solution by some iteration procedure. If this is the case, it is plausible that the solution is unique if  $\text{Re}\alpha_0, r(t_0)$  and the location of any possible zeroes in  $r(t)$  is given. These and other properties of the integral equation (2.15) for  $\text{Im}\alpha(t)$  are discussed in Sec. III. Here we shall proceed directly to a derivation of the integral equations which govern  $\text{Im}\alpha(t)$  in case a fermion Regge pole is exchanged in the  $t$  channel.

We shall consider Regge poles in the partial-wave amplitudes  $f_{\pm}(J,W)$ ,  $W=\sqrt{t}$ , which describe transitions in states of definite total angular momentum  $J=l\pm\frac{1}{2}$  and orbital angular momentum  $l$ . These amplitudes have the following symmetry<sup>13,14</sup>:

$$f_+(J, -W) = -f_-(J,W). \quad (2.17)$$

Accordingly, the Regge pole parameters connected with  $f_{\pm}(J,W)$  satisfy<sup>15,16</sup>

$$\alpha_+(-W) = \alpha_-(W) \quad (2.18)$$

and

$$r_+(-W) = -r_-(W). \quad (2.19)$$

The function  $\alpha_+(W)$  is real analytic and satisfies a dispersion relation<sup>15</sup>

$$\alpha_+(W) = \alpha_+(W_0) + \frac{W-W_0}{\pi} \int_{W_T}^{\infty} \frac{\text{Im}\alpha_+(W')dW'}{(W'-W)(W'-W_0)} - \frac{W-W_0}{\pi} \int_{W_T}^{\infty} \frac{\text{Im}\alpha_-(W')dW'}{(W'+W)(W'+W_0)}, \quad (2.20)$$

where  $W_T=(m_a+m_b)$  is the total c.m. threshold of the system and  $W_0$  the energy at the point of subtraction. In writing this dispersion relation, we have ignored the branch cuts arising from the crossing<sup>11</sup> of the trajectories  $\alpha_+$  and  $\alpha_-$ .

The unitarity condition satisfied by these amplitudes is of the form

$$[f_{\pm}(J,W) - f_{\pm}^*(J^*,W)]/2i = qf_{\pm}^*(J^*,W)f_{\pm}(J,W), \quad W > W_T. \quad (2.21)$$

$$r_+(W) = \frac{E+m_a}{W} (q^2)^{\alpha_+(W_0)-\frac{1}{2}} F(W) \exp \left[ -\frac{W-W_0}{\pi} \int_{W_T}^{\infty} \frac{\ln(q'^2/q^2)}{(W'-W)(W'-W_0)} \text{Im}\alpha_+(W')dW' + \frac{W-W_0}{\pi} \int_{W_T}^{\infty} \frac{\ln(q'^2/q^2)}{(W'+W)(W'+W_0)} \text{Im}\alpha_-(W')dW' \right], \quad (2.28)$$

We approximate the unitarity condition (2.21) by

$$r_{\pm}(W+i\epsilon) = (1/q) \text{Im}\alpha_{\pm}(W+i\epsilon), \quad W > W_T. \quad (2.22)$$

The functions  $f_{\pm}(J,W)$  have kinematic singularities and, as a result, the functions  $r_{\pm}(W)$  have kinematic singularities. However, the functions

$$h_{\pm}(J,W) = \frac{W}{E \pm m_a} \frac{f_{\pm}(J,W)}{(q^2)^{J-\frac{1}{2}}}, \quad (2.23)$$

where  $E$  is the energy of the particle  $a$

$$E = \frac{W^2 + m_a^2 - m_b^2}{2W},$$

do not have kinematic singularities.<sup>16</sup> Therefore, the functions  $(W/E \pm m_a)r_{\pm}(W)/(q^2)^{\alpha(W)-\frac{1}{2}}$  are real analytic in the  $W$  plane, with branch cuts from  $W_T$  to  $\infty$  and from  $-\infty$  to  $-W_T$ . Consequently, we have

$$r_{\pm}(W-i\epsilon) = r_{\pm}(W-i\epsilon)e^{2\pi i(\alpha_{\pm}(W-i\epsilon)-\frac{1}{2})}. \quad (2.24)$$

Let us consider the amplitude  $h_+(J,W)$ . As before, we write

$$\frac{W}{E+m_a} \frac{r_+(W)}{(q^2)^{\alpha_+(W)-\frac{1}{2}}} = F(W)e^{U(W)}, \quad (2.25)$$

where  $F(W)$  is an entire function of  $W$  and  $U(W)$  is analytic in  $W$  cut from  $W_T$  to  $\infty$  and from  $-\infty$  to  $-W_T$ . We obtain

$$U(W+i\epsilon) - U(W-i\epsilon) = -2i \text{Im}\alpha_+(W+i\epsilon) \ln q^2, \quad W > W_T \quad (2.26a)$$

and

$$U(W+i\epsilon) - U(W-i\epsilon) = 2i \text{Im}\alpha_-(-W+i\epsilon) \ln |q^2|, \quad W < -W_T. \quad (2.26b)$$

The above equations give

$$U(W) = -\frac{W-W_0}{\pi} \int_{W_T}^{\infty} \frac{\text{Im}\alpha_+(W') \ln q'^2}{(W'-W)(W'-W_0)} dW' + \frac{W-W_0}{\pi} \int_{W_T}^{\infty} \frac{\text{Im}\alpha_-(W') \ln q'^2}{(W'+W)(W'+W_0)} dW'. \quad (2.27)$$

From (2.25), (2.26), and (2.27) we get

<sup>13</sup> S. W. MacDowell, Phys. Rev. **116**, 774 (1960).

<sup>14</sup> W. Frazer and J. Fulco, Phys. Rev. **119**, 1420 (1960).

<sup>15</sup> V. N. Gribov, Zh. Eksperim. i Teor. Fiz. **43**, 1529 (1962) [translation: Soviet Phys.—JETP **16**, 1080 (1963)].

<sup>16</sup> V. Singh, Phys. Rev. **129**, 1889 (1963); N. Dombey (private communication).

and

$$\text{Im}\alpha_+(W) = \left(\frac{E+m_a}{W}\right) (q^2)^{\alpha_+(W_0)} F(W) \exp \left[ -\frac{W-W_0}{\pi} \int_{W_T}^{\infty} \frac{\ln(q'^2/q^2)}{(W'-W)(W'-W_0)} \text{Im}\alpha_+(W') dW' \right. \\ \left. + \frac{W-W_0}{\pi} \int_{W_T}^{\infty} \frac{\ln(q'^2/q^2)}{(W'+W)(W'+W_0)} \text{Im}\alpha_-(W') dW' \right], \quad W > W_T. \quad (2.29)$$

Also, we have

$$r_-(W) = -r_+(-W) \\ = -\left(\frac{E-m_a}{W}\right) (q^2)^{\alpha_+(W_0)-\frac{1}{2}} F(-W) \exp \left[ \frac{W+W_0}{\pi} \int_{W_T}^{\infty} \frac{\ln(q'^2/q^2)}{(W'+W)(W'-W_0)} \text{Im}\alpha_+(W') dW' \right. \\ \left. - \frac{W+W_0}{\pi} \int_{W_T}^{\infty} \frac{\ln(q'^2/q^2)}{(W'-W)(W'+W_0)} \text{Im}\alpha_-(W') dW' \right], \quad (2.30)$$

and

$$\text{Im}\alpha_-(W) = -\left(\frac{E-m_a}{W}\right) (q^2)^{\alpha_+(W_0)} F(-W) \exp \left[ \frac{W+W_0}{\pi} \int_{W_T}^{\infty} \frac{\ln(q'^2/q^2)}{(W'+W)(W'-W_0)} \text{Im}\alpha_+(W') dW' \right. \\ \left. - \frac{W+W_0}{\pi} \int_{W_T}^{\infty} \frac{\ln(q'^2/q^2)}{(W'-W)(W'+W_0)} \text{Im}\alpha_-(W') dW' \right], \quad W > W_T. \quad (2.31)$$

The function  $F(W)$  is a polynomial of order  $n$  in  $W$ , and satisfies

$$n + 2\alpha_+(\infty) < 0,$$

and, hence, can be written as

$$F(W) = \frac{W_0}{E_0 + m_a} \frac{1}{(q^2)^{\alpha_+(W_0)-\frac{1}{2}}} r_+(W_0) \prod_{i=1}^n \left( \frac{W - Z_i}{W_0 - Z_i} \right),$$

where  $Z_i$  are the zeroes of  $r_+(W)$ .

We thus obtain the following set of coupled integral equations to solve for  $\text{Im}\alpha_{\pm}(W)$ :

$$\text{Im}\alpha_+(W) = \frac{W_0}{W} \frac{E+m_a}{E_0+m_a} q (q^2/q_0^2)^{\alpha_+(W_0)-\frac{1}{2}} r_+(W_0) \prod_{i=1}^n \left( \frac{W - Z_i}{W_0 - Z_i} \right) \\ \times \exp \left\{ -\frac{W-W_0}{\pi} \int_{W_T}^{\infty} \ln \left( \frac{q'^2}{q^2} \right) \left[ \frac{\text{Im}\alpha_+(W')}{(W'-W)(W'-W_0)} - \frac{\text{Im}\alpha_-(W')}{(W'+W)(W'+W_0)} \right] dW' \right\}, \quad W > W_T, \quad (2.32)$$

$$\text{Im}\alpha_-(W) = -\frac{W_0}{W} \frac{E-m_a}{E_0+m_a} q (q^2/q_0^2)^{\alpha_+(W_0)-\frac{1}{2}} r_+(W_0) \prod_{i=1}^n \left( \frac{Z_i + W}{Z_i - W_0} \right) \\ \times \exp \left\{ \frac{W+W_0}{\pi} \int_{W_T}^{\infty} \ln \left( \frac{q'^2}{q^2} \right) \left[ \frac{\text{Im}\alpha_+(W')}{(W'+W)(W'-W_0)} - \frac{\text{Im}\alpha_-(W')}{(W'-W)(W'+W_0)} \right] dW' \right\}, \quad W > W_T. \quad (2.33)$$

Given  $\text{Im}\alpha_{\pm}(W)$ , we may obtain the functions  $r_{\pm}(W)$  from (2.28) and (2.30).

### III. FORMULATION AND DISCUSSION OF A SET OF INTEGRAL EQUATIONS FOR THE REGGE PARAMETERS: POTENTIAL THEORY CASE

In this section we shall turn to the formulation of a set of integral equations for the Regge parameters in the case when the scattering may be described by a superposition of Yukawa potentials. This topic is of interest because the most clear-cut check on the validity of our approximate form of the unitarity condition comes from a comparison of our results for the Regge parameters, computed for a single Yukawa potential, with the existing results found by numerically solving the Schrödinger equation.<sup>8</sup> Secondly, we can establish, in this case, several rather precise theorems regarding the properties of the integral equation which we shall derive for  $\text{Im}\alpha(\nu)$ . Here,  $\nu = k^2$  is the energy.

We recall that  $\alpha(\nu)$  and  $r(\nu)/\nu^{\alpha(\nu)}$  are both real analytic functions of  $\nu$  cut from 0 to  $\infty$ , when crossing of trajectories is neglected. The approximate form for the unitarity condition reads

$$r(\nu) = \text{Im}\alpha(\nu)/\sqrt{\nu}. \tag{3.1}$$

Writing

$$r(\nu)/\nu^{\alpha} = F(\nu)e^{U(\nu)}$$

and applying the same procedure as in the relativistic case, we obtain

$$\text{Im}\alpha(\nu) = r(\nu_0)\nu^{1/2} \left(\frac{\nu}{\nu_0}\right)^{\alpha_0} \prod_{i=1}^n \left(\frac{\nu-\nu_i}{\nu_0-\nu_i}\right) \exp\left[-\frac{(\nu-\nu_0)}{\pi} \int_0^{\infty} \frac{\ln(\nu'/\nu)}{(\nu'-\nu)(\nu'-\nu_0)} \text{Im}\alpha(\nu')d\nu'\right], \quad \nu > 0, \tag{3.2}$$

and

$$r(\nu) = r(\nu_0) \left(\frac{\nu}{\nu_0}\right)^{\alpha_0} \prod_{i=0}^n \left(\frac{\nu-\nu_i}{\nu_0-\nu_i}\right) \exp\left[-\frac{(\nu-\nu_0)}{\pi} \int_0^{\infty} \frac{\ln(\nu'/\nu)}{(\nu'-\nu)(\nu'-\nu_0)} \text{Im}\alpha(\nu')d\nu'\right], \tag{3.3}$$

where  $\nu_0$  denotes the point of subtraction and  $\nu_i, i=1, \dots, n$  gives the location of the zeroes of  $r(\nu)$ .

We would now like to show the relationship between the number of zeroes of  $r(\nu)$  and the asymptotic behavior of the Regge parameters.

From Eq. (3.2) we have

$$\text{Im}\alpha(\nu) \rightarrow \nu^{\alpha(\infty)+n+\frac{1}{2}}, \quad \nu \rightarrow \infty, \tag{3.4}$$

and

$$\text{Im}\alpha(\nu) \rightarrow \nu^{\alpha(0)+\frac{1}{2}}, \quad \nu \rightarrow 0. \tag{3.5}$$

Equation (3.4) shows that the number of zeroes is bounded by

$$n < -\alpha(\infty) - \frac{1}{2}, \tag{3.6}$$

and Eq. (3.5) gives the familiar threshold behavior of the Regge poles in the right-hand plane

$$\text{Re}\alpha(0) > -\frac{1}{2}. \tag{3.7}$$

Equation (3.6) is actually independent of our approximation. To prove this statement, we recall that  $r(\nu)/\nu^{\alpha(\nu)}$  is a real analytic function of  $\nu$  with cuts from 0 to  $\infty$  as well as those coming from the crossing of trajectories. We can therefore write

$$r(\nu) = \nu^{\alpha(\nu)} F(\nu) e^{U(\nu)} e^{W(\nu)}, \tag{3.8}$$

where  $U(\nu)$  is analytic in  $\nu$  cut from 0 to  $\infty$  and  $W(\nu)$  is analytic in  $\nu$  with cuts arising from crossing of trajectories. The functions  $U(\nu)$  and  $W(\nu)$  can be written in the form

$$U(\nu) = \frac{\nu-\nu_0}{\pi} \int_0^{\infty} \frac{1}{\nu'-\nu} \frac{\Delta U(\nu')}{(\nu'-\nu_0)} d\nu' \tag{3.9}$$

and

$$W(\nu) = \frac{\nu-\nu_0}{\pi} \int_c \frac{\Delta W(\nu')}{(\nu'-\nu)} \frac{d\nu'}{(\nu'-\nu_0)}, \tag{3.10}$$

where  $\Delta U(\nu)$  and  $\Delta W(\nu)$  are the discontinuities of  $U(\nu)$  and  $W(\nu)$  across the cut, and  $c$  is the contour of the cut arising from crossing of trajectories. If the trajectories cross at  $\nu_c$  and  $\nu_c$  is complex, then  $c$  is the straight line<sup>11</sup> going from  $\nu_c$  to  $\nu_c^*$  and

$$W(\nu) \xrightarrow{\nu \rightarrow \infty} -\frac{1}{\pi} \int_c \frac{\Delta W(\nu')}{\nu'-\nu_0} d\nu', \tag{3.11}$$

which is a finite number. If  $\nu_c$  is real, then the cut is from  $\nu_c$  to  $\infty$ . Now<sup>5,9,11</sup>

$$\text{Im}\alpha(\nu) \rightarrow -(g^2/2\sqrt{\nu}), \tag{3.12}$$

$$r(\nu) \rightarrow -(g^2/2\nu), \quad \nu \rightarrow \infty$$

and  $r(\nu)$  is real for  $\nu$  real. Thus,

$$\frac{r(\nu_+) \nu_+^{-\alpha(\nu_+)}}{r(\nu_-) \nu_-^{-\alpha(\nu_-)}} \rightarrow \exp[-2i \text{Im}\alpha(\nu) \ln \nu],$$

and, therefore,

$$\Delta U(\nu) + \Delta W(\nu) \rightarrow -2i \text{Im}\alpha(\nu) \ln \nu \text{ as } \nu \rightarrow \infty, \tag{3.13}$$

$\rightarrow 0.$

Thus, we have

$$U(\nu) + W(\nu) \rightarrow -\frac{1}{\pi} \left\{ \int_c \frac{\Delta W(\nu')}{\nu'-\nu_0} d\nu' + \int_0^{\infty} \frac{\Delta U(\nu')}{\nu'-\nu_0} d\nu' \right\}, \tag{3.14}$$

$\nu \rightarrow \infty,$

which is a finite number. Equations (3.8), (3.11), and (3.14) together give

$$r(\nu) \rightarrow \nu^{\alpha(\infty)+n}, \quad \nu \rightarrow \infty \tag{3.15}$$

where  $n$  is the number of zeroes of  $r(\nu)$ . Comparing (3.12) and (3.15), we conclude that

$$n = -\alpha(\infty) - 1. \tag{3.16}$$

The first Regge trajectory, having  $\alpha(\infty) = -1$ , therefore, has no zero, while the second, the third, . . . trajectories have one, two, . . . zeroes, respectively.

Now let us discuss Eq. (3.2) for the leading trajectory, which has no zero. Then we may write

$$U(\nu) = -\frac{r(\nu_0)}{\nu_0^{\alpha_0}} \frac{(\nu-\nu_0)}{\pi} \int_0^{\infty} \frac{\ln(\nu'/\nu)}{(\nu'-\nu)(\nu'-\nu_0)} \nu'^{\alpha_0+\frac{1}{2}} e^{U(\nu')} d\nu',$$

and

$$\text{Im}\alpha(\nu) = [r(\nu_0)/\nu_0^{\alpha_0}] \nu^{\alpha_0+\frac{1}{2}} e^{U(\nu)}, \quad \nu > 0. \tag{3.17}$$

If we take the subtraction point at  $\nu=0$ , then we obtain

$$U(\nu) = -\lambda \frac{\nu}{\pi} \int_0^{\infty} \frac{\ln(\nu'/\nu)}{(\nu'-\nu)} \nu'^{\alpha(0)-1/2} e^{U(\nu')} d\nu' \tag{3.17a}$$

and

$$\text{Im}\alpha(\nu) = \lambda \nu^{\alpha(0)+\frac{1}{2}} e^{U(\nu)}, \quad \nu > 0,$$

where

$$\lambda = \lim_{\nu \rightarrow 0} \frac{r(\nu)}{\nu^{\alpha(\nu)}}.$$

And, if we take the subtraction point at  $\nu = \infty$ , then we have

$$U(\nu) = -\frac{\lambda}{\pi} \int_0^\infty \frac{\ln(\nu'/\nu)}{(\nu' - \nu)} \nu'^{\alpha(\infty)+1/2} e^{U(\nu')} d\nu' \quad (3.17b)$$

and

$$\text{Im}\alpha(\nu) = \lambda \nu^{\alpha(\infty)+\frac{1}{2}} e^{U(\nu)}, \quad \nu > 0,$$

where

$$\lambda = \lim_{\nu \rightarrow \infty} \frac{r(\nu)}{\nu^{\alpha(\nu)}}.$$

We should like to point out several interesting consequences of Eqs. (3.17a) and (3.17b). We require  $\text{Im}\alpha(0) = 0$  and  $\text{Im}\alpha(\infty) = 0$ . Thus, the following inequalities have to be satisfied:

$$\alpha(0) > -\frac{1}{2} \quad (3.18a)$$

$$\alpha(\infty) < -\frac{1}{2}. \quad (3.18b)$$

If we take  $\alpha(\infty) = -1$ , which is correct for the leading trajectory, then (3.17b) shows that  $\text{Im}\alpha(\nu)$  has the correct asymptotic form as  $\nu \rightarrow \infty$ , providing  $\lambda = g^2/2$ . The solution of (3.17b), which is the equation having the subtraction point at  $\nu = \infty$ , should thus be expected to give a good approximation to  $\alpha(\nu)$  and  $r(\nu)$  at large  $\nu$ . For the same reason, the solution of (3.17a), which gives the correct threshold behavior, should approximate  $\alpha(\nu)$  and  $r(\nu)$  accurately at small  $\nu$ . It has been pointed out to the authors<sup>17</sup> that (3.17b) is dependent on the coupling constant  $g^2$  only and is independent of the range  $\mu$  of the potential. But (3.17b) is good only for  $\nu$  large, and when the energy is large the mass can usually be neglected. In fact, the asymptotic forms for  $\alpha(\nu)$  and  $\beta(\nu)$  have been shown to be independent of  $\mu$ . It is therefore natural that the range of the potential does not enter in (3.17b). On the other hand, if we make a subtraction at  $\nu = 0$ , or at some point  $\nu_0$  near zero, then the solution will be accurate at low energy if the subtraction constants  $\alpha(\nu_0)$  and  $r(\nu_0)$  are both supplied. It should be noticed that if we make a subtraction at some finite point  $\nu_0$ , then the solution of (3.17) would not automatically give  $\alpha(\infty) = -1$ , in disagreement with the known behavior of the trajectory. However, in this case, we expect the solution to be accurate only at *low* energy, and its behavior at  $\nu = \infty$  cannot, in general, be expected to be given in a precisely correct way using our approximate equations.

Suppose we have two functions  $U^{(1)}(\nu)$  and  $U^{(2)}(\nu)$  satisfying (3.17a) with different subtraction constants

$\lambda_1$  and  $\lambda_2$  but the same subtraction constant  $\alpha(0)$ . Then a change of variable shows that

$$U^{(1)}\left(\frac{\nu}{[\lambda_1]^{\alpha(0)+1/2}}\right) = U^{(2)}\left(\frac{\nu}{[\lambda_2]^{\alpha(0)+1/2}}\right) \quad (3.19)$$

and as a result

$$\alpha^{(1)}\left(\frac{\nu}{[\lambda_1]^{\alpha(0)+1/2}}\right) = \alpha^{(2)}\left(\frac{\nu}{[\lambda_2]^{\alpha(0)+1/2}}\right). \quad (3.20)$$

In particular, we have

$$\alpha^{(1)}(\infty) = \alpha^{(2)}(\infty). \quad (3.21)$$

Thus, we see that  $\alpha(\infty)$  is determined by the subtraction constant  $\alpha(0)$  and is independent of  $\lambda$ . Similarly, the solutions of (3.17b) give the same  $\alpha(0)$ , if  $\alpha(\infty)$  is fixed and  $\lambda$  is varied, and equalities similar to (3.19) and (3.20) hold.

Now let us turn to the question of the existence of a solution of Eq. (3.17a) or (3.17b). First, it is clear that because of Eqs. (3.19) and (3.20), if there is a solution of Eq. (3.17a) for a certain  $\lambda$  and  $\alpha(0)$ , then there is always a solution of Eq. (3.17a) for an arbitrary  $\lambda$  and the same  $\alpha(0)$ . The same is true for (3.17b). The question of existence and uniqueness of a solution depends on the subtraction constant  $\alpha(0)$  [or  $\alpha(\infty)$ ] only. Secondly, (3.17a) does *not* have a solution for an arbitrary  $\alpha(0)$ . A necessary condition for the existence of a solution of Eq. (3.17a) is Eq. (3.18a). For, if there is a solution of Eq. (3.17a), then  $U(0) = 0$ , and the integral on the right side of (3.17a) does not converge at the end point  $\nu' = 0$  unless (3.18a) is satisfied. Similarly, a necessary condition for the existence of a solution of Eq. (3.17b) is (3.18b).

Some precise theorems on the existence and uniqueness of the solutions of Eqs. (3.17a, b) can be proved<sup>18</sup> if certain conditions on the subtraction constants are satisfied.

#### IV. REGGE POLE PARAMETERS FOR A SINGLE YUKAWA POTENTIAL. PRESENTATION AND DISCUSSION OF RESULTS

The Regge pole parameters associated with a single Yukawa potential of unit range have been obtained by Ahmadzadeh, Burke, and Tate<sup>8</sup> and by Lovelace and Masson,<sup>9</sup> for several potential strengths. Ahmadzadeh *et al.*<sup>8</sup> obtained their results by solving the Schrödinger equation numerically, while Lovelace and Masson<sup>9</sup> used a continued fraction technique applied to the known<sup>5,9,11</sup> form (in *potential* theory) of the asymptotic ( $k^2 \rightarrow \infty$ ) expansions of the Regge parameters.

A comparison of the Regge parameters as calculated using Eq. (3.2) of the preceding section with the results of Ahmadzadeh *et al.*<sup>8</sup> and Lovelace and Masson<sup>9</sup> provides an important test of the accuracy of our ap-

<sup>17</sup> M. Gell-Mann and F. Zachariasen (private communication).

<sup>18</sup> H. Cheng (to be published).

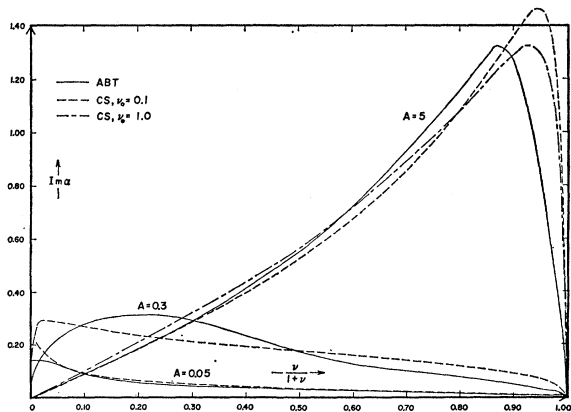


FIG. 1.  $\text{Im}\alpha(\nu)$  versus  $\nu/(1+\nu)$ ,  $0 < \nu < \infty$ . The results of this work are compared with those of Ahmadzadeh *et al.* (Ref. 8) for single attractive Yukawa potentials of unit range and strengths  $A=0.05, 0.30$ , and  $5$ . In our equations, subtractions have been made at  $\nu_0=1.0$  and  $0.1$  for the case  $A=5$ , and at  $\nu_0=0.1$  for the case  $A=0.05$  and  $0.3$ . Here,  $\nu=k^2$ .

proximation. This section contains such a comparison.

Our procedure was to use the results of Refs. 8 and 9 to supply the value of  $\alpha(\nu)$  and  $\beta(\nu)$  at a subtraction point  $\nu_0$ . [We actually obtain  $\beta(\nu_0)$  from  $\text{Im}\alpha(\nu_0)$  and the unitarity condition (3.1).] Then we solve Eqs. (3.2) and (2.1) numerically<sup>19</sup> for the functions  $\text{Im}\alpha(\nu)$  and  $\text{Re}\alpha(\nu)$  as functions of  $\nu$  for  $\nu$  in the range  $-\infty < \nu < \infty$ . A solution could always be obtained after a few iterations if we used the average value of the input and output functions as the next input.

The results for several values of the potential strength  $A$  are presented and compared with the results of Refs. 8 and 9 in Figs. 1-8. Results for  $\text{Im}\alpha(\nu)$  are presented for the range  $\nu=0 \rightarrow \infty$  and for  $\text{Re}\alpha(\nu)$  for the range  $\nu=-2 \rightarrow +\infty$ .

Let us consider some individual curves. In the case of strong coupling,  $A=5$  and  $15$ , we see from Figs. 1-4 that we obtain quite good qualitative and quantitative agreement between our results and those of Refs. 8 and 9 over the entire range of energy. Note that in the case  $A=5$ , results are presented for two different subtraction points. The solutions are essentially the same. We would like to mention also that if we have obtained  $\text{Im}\alpha(\nu)$  correctly,  $\text{Re}\alpha(\nu)$  must also be given correctly, subject to the assumptions: (a) that  $\alpha(\nu)$  is a real analytic function; (b) that the trajectory considered does not cross with other trajectories; and (c) that the Hilbert transform has been performed without significant numerical error.

Next, we consider curves in the regime of intermediate coupling,  $A=1, 1.8$ , and  $3$ . For the case  $A=3$ , Figs. 5

<sup>19</sup> In solving these equations numerically, we have used an "on-line" computing center as developed by Dr. G. J. Culler and Dr. B. D. Fried of the Thomson-Ramo-Wooldridge Corporation. This system has proved to be of particular value in our problem in instances where it was difficult to devise a convergent iteration scheme. For a detailed description of their computing facility, see G. J. Culler and B. D. Fried, Ramo-Wooldridge Research Laboratory report, January 1963 (unpublished).

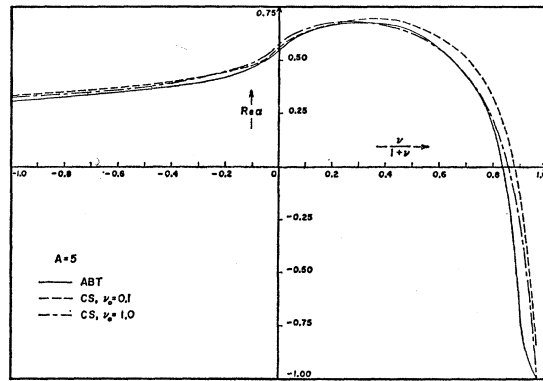


FIG. 2.  $\text{Re}\alpha(\nu)$  versus  $\nu/(1+\nu)$ ,  $-2 < \nu < \infty$ . Results for potential strength  $A=5$  compared with those of Ahmadzadeh *et al.* (Ref. 8) See caption of Fig. 1.

and 6, the solution obtained has an accuracy comparable to that found in the strong-coupling case. For the case  $A=1.8$ , Figs. 7 and 8, we find a case in which we obtain our poorest agreement, but the solution still possesses the correct qualitative shape, and is quantitatively accurate in a region around the subtraction point. The case  $A=1$  shows the same general features (Figs. 5 and 6).

Turning now to the weak-coupling cases,  $A=0.05$  and  $0.30$ , we find the agreement much improved. In the case  $A=0.05$ , Fig. 1, the agreement for the  $\text{Im}\alpha$  curve is fully comparable to that obtained in the strong coupling cases, with the exception of the region  $0 < (\nu/1+\nu) < 0.05$ . We understand the departure of the curves in this region from the correct ones to be due to limitations on the numerical accuracy with which we carried out the integral transforms involved. This problem is extreme in these cases, because we find from Ref. 8 that in the case  $A=0.05$ ,  $\text{Im}\alpha(\nu)$  goes from 0 to  $\sim 0.10$  while  $\nu[\approx \nu/(1+\nu)$  for  $\nu \ll 1$ ] goes from 0 to  $10^{-3}$ . The value  $0.10$  represents  $\sim 60\%$  of its peak value. Our program could not handle such rapid changes ac-

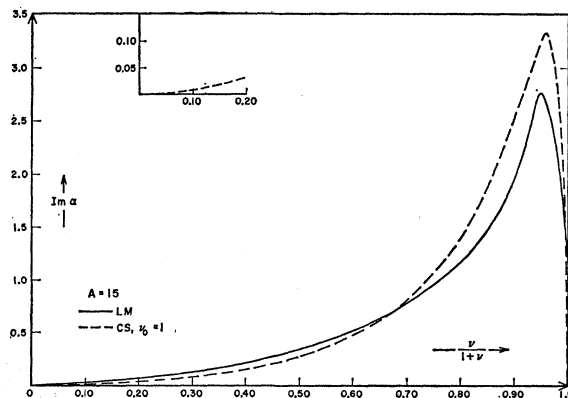


FIG. 3.  $\text{Im}\alpha(\nu)$  versus  $\nu/(1+\nu)$ ,  $0 < \nu < \infty$ . Comparison of the results of this work with those of Lovelace and Masson (Ref. 9) for a single Yukawa potential of unit range and strength  $A=15$ . The point of subtraction was  $\nu_0=1.0$ . Here,  $\nu=k^2$ .



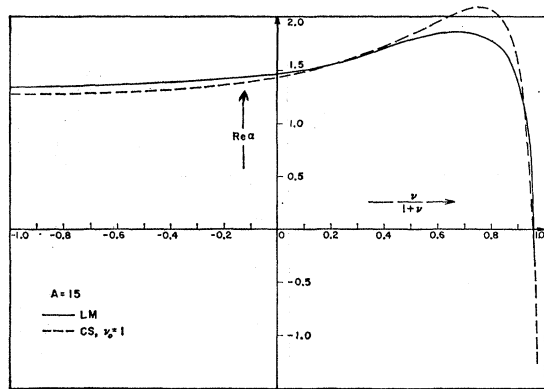


FIG. 4.  $\text{Re}\alpha(\nu)$  versus  $\nu/(1+\nu)$ ,  $-2 < \nu < \infty$ . Results for potential strength  $A=15$  compared with those of Lovelace and Masson (Ref. 9). See caption of Fig. 3.

curately, although this situation could no doubt be improved. Similar remarks apply to the case  $A=0.3$  (Fig. 1).

We do not understand why our approximation should be so much better in the strong- and weak-coupling cases than in the intermediate coupling case. One possibility is that the intermediate coupling region is one in which the first and second Regge trajectories for a given coupling strength cross. If this is the case, then the dynamical equations for the Regge parameters in the form we have used them here are not correct.<sup>7,11</sup>

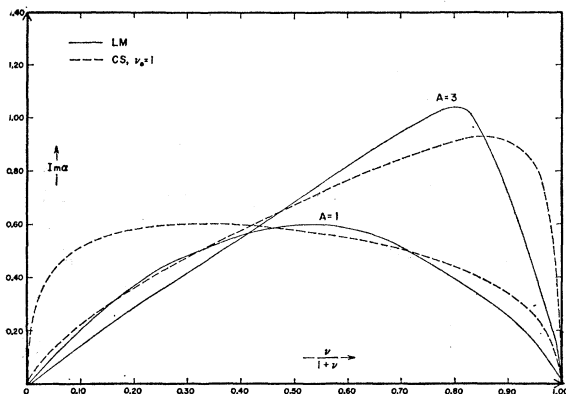


FIG. 5.  $\text{Im}\alpha(\nu)$  versus  $\nu/(1+\nu)$ ,  $0 < \nu < \infty$ . Results of this work compared with those of Lovelace and Masson (Ref. 9) for single Yukawa potentials of unit range and strengths  $A=1$  and  $A=3$ . The point of subtraction was  $\nu_0=1$ . Here,  $\nu=k^2$ .

However, we have no evidence that such crossings are, in fact, responsible for the disagreement.

An interesting fact is that the curves  $\text{Re}\alpha(\nu)$ , for  $\nu \rightarrow \infty$ , all approach negative values fairly close to  $-1$  in good agreement with the asymptotic behavior of  $\text{Re}\alpha(\nu)$  which has been proven rigorously.<sup>5,9,11</sup> [ $A=5$ ,  $\text{Re}\alpha(\infty) \sim -1.39$ ;  $A=3$ ,  $\text{Re}\alpha(\infty) \sim -1.29$ ;  $A=1.8$ ,  $\text{Re}\alpha(\infty) \sim -0.75$ ,  $-1.05$ ;  $A=1.0$ ,  $\text{Re}\alpha(\infty) \sim -1.19$ ; exception  $A=15$ ,  $\text{Re}\alpha(\infty) \sim -2.66$ .] This result was

obtained without making any explicit assumption about the asymptotic behavior of  $\text{Re}\alpha$ .

The function  $r(\nu)$  obtained from our equation, in the case  $A=5$ , was compared with that obtained by Ahmadzadeh, Burke, and Tate.<sup>8</sup> The curves have a reasonably correct shape, and there is quantitative agreement in the low-energy region.

To summarize, we feel that the results presented here support the following general conclusions in the case of potential theory:

(1) Our equations provide a dynamical determination of the Regge parameters which always gives the correct

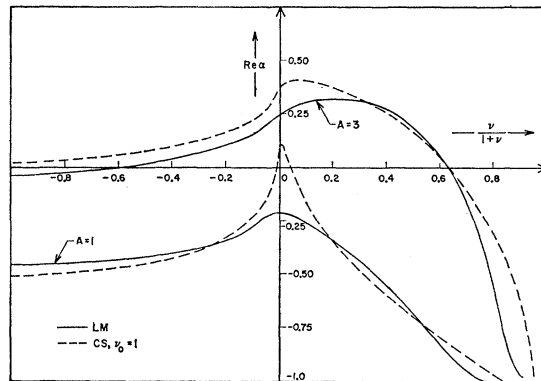


FIG. 6.  $\text{Re}\alpha(\nu)$  versus  $\nu/(1+\nu)$ ,  $-2 < \nu < \infty$ . Results for potential strengths  $A=1$  and  $3$  compared with those of Lovelace and Masson (Ref. 9). See caption of Fig. 5.

shape of the curves, and gives quantitatively correct results in the neighborhood of the subtraction point.

(2) In case the coupling of the Regge poles is strong or weak, we get good quantitative agreement over a considerable range of energy.

Finally, we emphasize that our equation has been tested for the leading trajectories only, which have no zeroes. It will be interesting to see if our equation yields

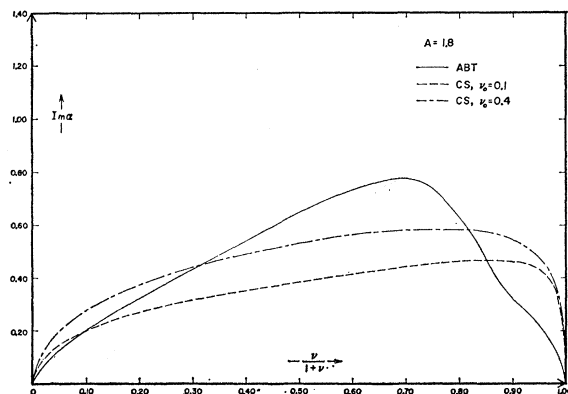


FIG. 7.  $\text{Im}\alpha(\nu)$  versus  $\nu/(1+\nu)$ ,  $0 < \nu < \infty$ . Results of this work compared with those of Ahmadzadeh *et al.* (Ref. 8) for a single Yukawa potential of unit range and strength  $A=1.8$ . Subtractions were made at the energies  $\nu_0=0.1$  and  $\nu_0=0.4$ . Here,  $\nu=k^2$ .

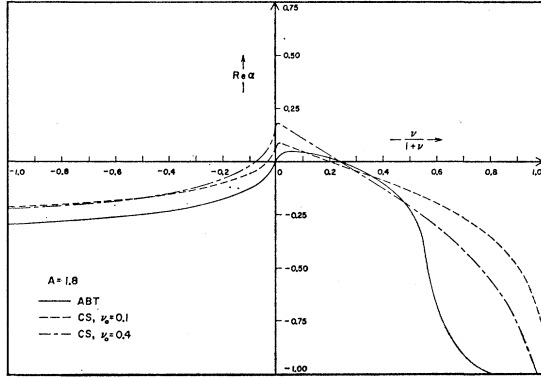


FIG. 8.  $Re\alpha_p(\nu)$  versus  $\nu/(1+\nu)$ ,  $-2 < \nu < \infty$ . Our results for a potential strength  $A=1.8$  compared with those of Ahmadzadeh *et al.* (Ref. 8). See caption of Fig. 7.

accurate solutions for other trajectories which have zeroes and for which  $\alpha(0) > -\frac{1}{2}$ .

V. THE REGGE POLE PARAMETERS IN RELATIVISTIC  $\pi\pi$  SCATTERING

In this section, we shall apply the equations derived in Sec. II to discuss elastic  $\pi\pi$  scattering at high energies. We will consider the contributions to this scattering of the Pomeranchuk trajectory, which has the quantum numbers of the vacuum and  $\alpha_p(0)=1$ , and the  $\rho$  trajectory which gives a  $2\pi$  ( $J=1, I=1$ ) resonance at 750 MeV. We shall also briefly discuss the second

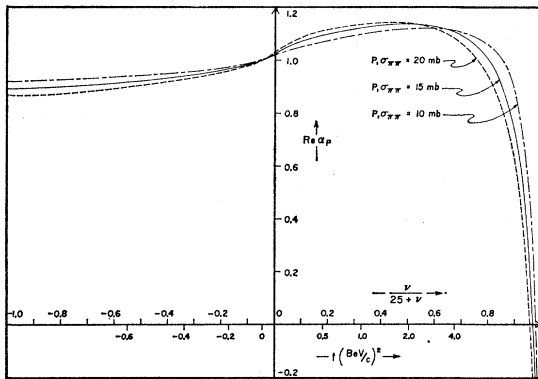


FIG. 9. Pomeranchuk trajectory.  $Re\alpha_p(t)$  versus  $t$ ,  $-0.80 \times (\text{BeV}/c)^2 < t < \infty$ . The three curves shown are calculated using the input parameters: (a)  $\alpha_p(0)=1, \sigma_{\pi\pi}(\infty)=10$  mb; (b)  $\alpha_p(0)=1, \sigma_{\pi\pi}(\infty)=15$  mb; and (c)  $\alpha_p(0)=1, \sigma_{\pi\pi}(\infty)=20$  mb.

vacuum trajectory  $P'$  introduced by Igi.<sup>10</sup> Since direct measurements of the  $\pi\pi$ -scattering cross sections are not yet available, we have concentrated here on obtaining the positions  $\alpha(t)$  of these trajectories, which functions will then occur in all reactions having the proper quantum numbers.

We shall first discuss the Pomeranchuk trajectory. Its Regge pole parameters will be determined by Eqs. (2.1) and (2.15) which, as we have mentioned, couple the Pomeranchuk trajectory only to itself.

Our procedure was to supply as input parameters the quantities  $\alpha_p(0)=1$  and<sup>20</sup>

$$\sigma_{\pi\pi}(\infty) = -(4\pi^2/3)[2\alpha_p(0)+1]r_p(0),$$

and solve the equation for  $Im\alpha_p$  by an iteration procedure which takes the average value of the input and output functions as the next input. Then  $Re\alpha_p(t)$  was obtained from the dispersion relation (2.1).

We have obtained solutions for  $\sigma_{\pi\pi}(\infty)$  in the range  $30 \rightarrow 30$  mb. The results for  $Re\alpha_p(t)$  and  $Im\alpha_p(t)$  for  $\sigma_{\pi\pi}(\infty)=10, 15,$  and  $20$  mb are shown in Figs. 9 and 10. In Fig. 11, our results for  $Re\alpha_p(t)$ , for  $-0.8(\text{BeV}/c)^2$

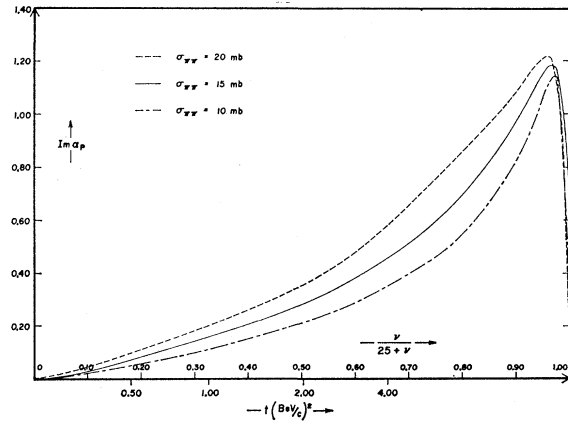
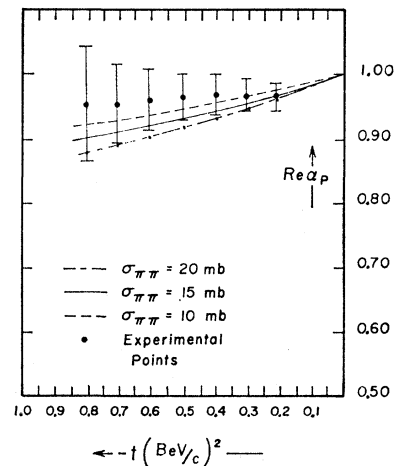


FIG. 10. Pomeranchuk trajectory.  $Im\alpha_p(t)$  versus  $t, 0.08 (\text{BeV}/c)^2 < t < \infty$ . The three curves shown were calculated using the input parameters listed in the caption of Fig. 9.

$< t < 0$ , are compared with those obtained by Foley *et al.*<sup>1</sup> from an analysis of the  $\pi^-p$  angular distributions measured at incident momenta in the range 7 to 17 BeV/c, and for the above-mentioned range of  $t$ .

It will be noted that our  $Re\alpha_p$  curves fall within the error flags around the experimental points measured by Foley *et al.*<sup>1</sup> We feel that this agreement is reasonably

FIG. 11. Comparison of  $Re\alpha(t)$  for the Pomeranchuk trajectory as computed in this paper (input parameters;  $\alpha_p(0)=1, \sigma_{\pi\pi}(\infty)=10, 15, 20$  mb) with  $Re\alpha(t)$  as determined by Foley *et al.* (Ref. 1) from an analysis of  $\pi^-p$  angular distributions for incident momenta in the range 7 BeV/c to 17 BeV/c and  $-0.80(\text{BeV}/c)^2 < t < -0.20(\text{BeV}/c)^2$ .



<sup>20</sup> This relation is derived in the Appendix.

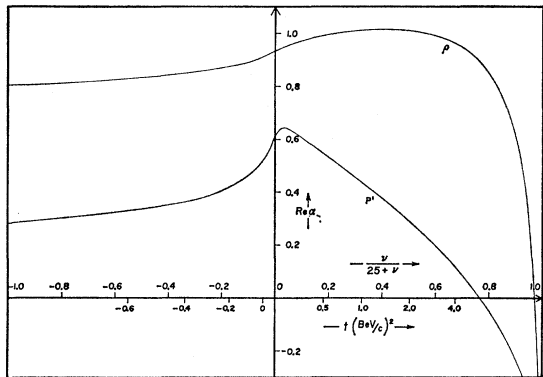


FIG. 12.  $P'$  trajectory and  $\rho$ -meson trajectory.  $\text{Re}\alpha_{P'}(t)$  versus  $t$ ,  $\text{Re}\alpha_{\rho}(t)$  versus  $t$ ,  $-0.8(\text{BeV}/c)^2 < t < \infty$ . The input parameter; were: (a) For the  $P'$ ;  $\alpha_{P'}(0)=0.50$ ,  $\sigma_{\pi\pi}^{P'}(s)$  ( $s \approx 20(\text{BeV})^2$ ) = 5 mb; (b) for the  $\rho$ ,  $\text{Re}\alpha_{\rho}(m_{\rho}^2)=1$ ,  $\text{Im}\alpha_{\rho}(m_{\rho}^2)=0.10$ .

significant because the region where the comparison is made is very close to the subtraction point ( $t=0$ ), which is, of course, the region in which our results are most reliable. Secondly, the results are not extremely sensitive to the value of the input parameter  $\sigma_{\pi\pi}(\infty)$ .

The fact that our result for  $\text{Re}\alpha_{\rho}$  agrees with that of Foley *et al.*<sup>1</sup> naturally implies that it disagrees with  $\text{Re}\alpha_{\rho}$  as it has so far been determined from an analysis of  $NN$  scattering data.<sup>1,3</sup>

We do not have a resolution of this puzzle. However, we do feel that it is more likely that the  $\pi N$  rather than the  $NN$  angular distributions are dominated by the Pomeranchuk trajectory. The reason for this is that the statement that the Pomeranchuk trajectory dominates  $NN$  scattering, which depends on the assumption of a cancellation of large contributions from the  $P'$  and  $\omega$  (or perhaps  $\phi$ ) trajectories,<sup>21,22</sup> is much more model-dependent than the conjecture that it dominates  $\pi N$  scattering.

We note from Fig. 9 that  $\text{Re}\alpha_{\rho}(t)$  does not pass through 2 for any value of  $t$ . This implies that there is no spin-2 resonance on the Pomeranchuk trajectory. However, it may well be that the inclusion of inelastic states could change this conclusion. Moreover, the region where the curves peak [ $t \sim 2$  or  $3 (\text{BeV}/c)^2$ ] is rather far away from the subtraction point, which may result in further inaccuracies.

We have also obtained solutions for the  $P'$  trajectory,<sup>10</sup> assuming  $\alpha_{P'}(0)=\frac{1}{2}$  and, quite arbitrarily, that at  $t=0$  and  $s \sim 20 (\text{BeV})^2$  it contributes 5 mb to the total  $\pi\pi$  cross section. Results are shown in Figs. 12 and 13. It is of interest to note that  $\text{Re}\alpha_{P'}$  falls off considerably faster for negative  $t$  than does the Pomeranchuk trajectory, and that it reaches its peak value at a much lower energy [ $t \sim 0.15 (\text{BeV}/c)^2$ ].

Lastly, we have obtained solutions for the  $\rho$  trajectory.

TABLE I. A list of values of  $\Gamma_{\rho}$  and  $\alpha_{\rho}(0)$  for input parameters  $\alpha_{\rho}(m_{\rho}^2)=1$  and  $\text{Im}\alpha_{\rho}(m_{\rho}^2)$ .

$\text{Im}\alpha_{\rho}(m_{\rho}^2)$	$\Gamma_{\rho} = \frac{\text{Im}\alpha_{\rho}(m_{\rho}^2)}{m_{\rho}\epsilon_{\rho}(m_{\rho}^2)}$	$\alpha_{\rho}(0)$
0.005	$3.79 m_{\pi}$	0.990
0.010	$4.45 m_{\pi}$	0.983
0.025	$6.35 m_{\pi}$	0.966
0.100	$18.9 m_{\pi}$	0.913

In this case, we solved for the trajectories in the following way. We used the fact that  $\text{Re}\alpha_{\rho}(m_{\rho}^2)=1$  and then we chose a reasonable corresponding value of  $\text{Im}\alpha_{\rho}(m_{\rho}^2)$ . We then obtained a set of solutions corresponding to these parameters, computed  $\epsilon_{\rho}(m_{\rho}^2)$  and checked to see if the width as given by

$$m_{\rho}\Gamma_{\rho} = \text{Im}\alpha_{\rho}(m_{\rho}^2)/\epsilon_{\rho}(m_{\rho}^2), \quad (5.1)$$

where

$$\epsilon_{\rho}(m_{\rho}^2) = d \text{Re}\alpha_{\rho}/dt|_{t=m_{\rho}^2} \quad (5.2)$$

came out correctly. Using this trial and error procedure, we were not able to find a set of parameters which gave a precisely correct value for the  $\rho$  width.

In Figs. 12 to 15, we display our results for  $\text{Re}\alpha_{\rho}(t)$  and  $\text{Im}\alpha_{\rho}(t)$  for several values of the input parameter  $\text{Im}\alpha_{\rho}(m_{\rho}^2)$ . The corresponding values of the width and  $\alpha_{\rho}(0)$  are summarized in Table I.

It is to be noted that we obtain a very large value of  $\alpha_{\rho}(0)$ , and that we find  $\alpha_{\rho}(t) > 0.90$  for  $-0.80 (\text{BeV}/c)^2 < t < 0$  (Fig. 14). This fact is quite insensitive to the magnitude of the input parameter  $\alpha_{\rho}(m_{\rho}^2)$ . Thus, we feel that the numbers we obtain for  $\alpha_{\rho}(t)$ ,  $t=0$  or  $t \leq 0$ , may not be modified greatly by the inclusion of inelastic states. The value of  $\alpha_{\rho}(t)$ ,  $-0.80 (\text{BeV}/c)^2 < t < 0$ , that we find seems to be consistent with the recent observations of Lindenbaum *et al.*<sup>23</sup> who find little or no energy dependence of the  $\pi^{\pm}p$  angular distributions. This sug-

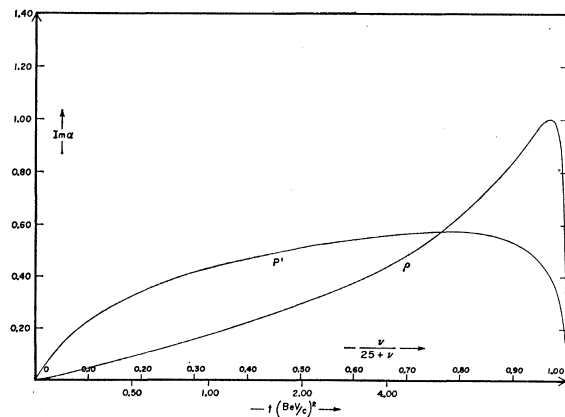


FIG. 13.  $P'$  trajectory and  $\rho$ -meson trajectory.  $\text{Im}\alpha_{P'}(t)$  versus  $t$ ;  $\text{Im}\alpha_{\rho}(t)$  versus  $t$ ,  $0.08(\text{BeV}/c)^2 < t < \infty$ . These curves were calculated with the input parameters listed in the caption of Fig. 12.

<sup>21</sup> F. Hadjiannou, R. J. N. Phillips, and W. Rarita, Phys. Rev. Letters **9**, 183 (1962).

<sup>22</sup> D. H. Sharp and W. G. Wagner, Phys. Rev. **131**, 2224 (1963).

<sup>23</sup> S. J. Lindenbaum (private communications).

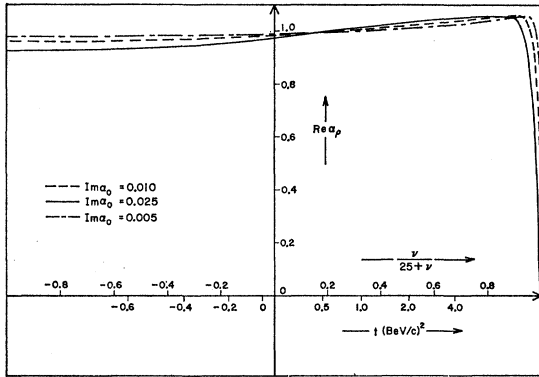


FIG. 14.  $\rho$ -meson trajectory.  $\text{Re}\alpha_\rho(t)$  versus  $t$ ,  $-0.8(\text{BeV}/c)^2 < t < \infty$ . The three curves shown were calculated from the input parameters: (a)  $\text{Re}\alpha_\rho(m_\rho^2)=1$ ,  $\text{Im}\alpha_\rho(m_\rho^2)=0.005$ ; (b)  $\text{Re}\alpha_\rho(m_\rho^2)=1$ ,  $\text{Im}\alpha_\rho(m_\rho^2)=0.010$ ; (c)  $\text{Re}\alpha_\rho(m_\rho^2)=1$ ,  $\text{Im}\alpha_\rho(m_\rho^2)=0.025$ .

gests that  $0.80 < \alpha_\rho(0) < 1$ , while we find typically  $\alpha_\rho(0) \sim 0.98$ . An analysis of earlier data<sup>24</sup> on the  $\pi^\pm p$  total cross sections, restricted to incident momenta greater than 10 BeV/c may also support the conclusion that  $\alpha_\rho(0)$  is  $\sim 0.80$  or larger.<sup>23</sup> Moreover, one should bear in mind that the  $\sigma_{np}$  data is so poor that a determination of  $\alpha_\rho(0) \sim 0.4$  from that data is without much statistical significance.<sup>25</sup>

The width of the  $\rho$  meson comes out too large by a factor of  $\sim 5$ , assuming  $\Gamma_\rho \sim 100$  MeV. This, no doubt, indicates that inelastic states must be included in order to obtain the  $\rho$  width correctly. This is probably not surprising in view of the results of other attempts to determine the  $\rho$  width dynamically.<sup>26</sup>

There is an additional complication that enters the determination of the widths from our Regge parameters. This is the fact that  $\epsilon_\rho(m_\rho^2)$  is a small difference of large quantities, and a very small percentage error in  $\text{Re}\alpha_\rho(\sim \frac{1}{2}\%)$  may result in very large errors in  $\epsilon_\rho(\sim 100\%)$ . This may account for some of the error in our value of the  $\rho$  width.

Finally, we would like to record that we found  $\text{Re}\alpha_\rho(\infty) \sim -0.66$  ( $\sigma_{\pi\pi} = 15$  mb);  $\text{Re}\alpha_{\rho'}(\infty) \sim -0.63$  and  $\text{Re}\alpha_\rho(\infty) \sim -0.56$  [ $\text{Im}\alpha_\rho(m_\rho^2) = 0.10$ ]. We have made no explicit assumption about the asymptotic behavior except that  $\text{Im}\alpha(t) \rightarrow 0$  as  $t \rightarrow \infty$ .

## VI. CONCLUSION

We have presented in this paper an approximate method for the dynamical determination of the Regge pole parameters. The equations we have derived for this purpose are simple in structure and rather easy to solve numerically.

<sup>24</sup> S. J. Lindenbaum, W. A. Love, J. A. Niederer, S. Ozaki, J. J. Russell, and L. C. L. Yuan, Phys. Rev. Letters 7, 352 (1961).

<sup>25</sup> V. I. Lendyel and J. Mathews (private communication).

<sup>26</sup> See, for example: F. Zachariasen and A. C. Zemach, Phys. Rev. 128, 849 (1962), who find  $\Gamma_\rho \sim 400$  MeV after including the contribution of  $\pi\omega$  intermediate states.

In the potential theory case, where a comparison with an exact solution is possible, the agreement is gratifying in most instances.

We do not understand why, in the nonrelativistic case, the accuracy of the solution obtained appears to be poorest when the potential strength is in the range  $1 \lesssim A \lesssim 3$ . It may mean that, for  $A$  in this range, the one-pole approximation is not adequate. Alternatively, this trajectory may cross another, in which case the equations must be formulated differently.<sup>11</sup>

In the relativistic case, the solutions obtained for the Pomernchuk trajectory agree quite well with the experimental results of Foley *et al.*<sup>1</sup> Our solutions for the  $\rho$  trajectory give a value of  $\alpha_\rho(0)$  which seems to be consistent with recent measurements of Lindenbaum *et al.*<sup>23</sup> However, we find that the width of the  $\rho$  resonance comes out too large. The inclusion of inelastic channels should improve the results. But whether we can achieve quantitatively accurate solutions by including just the two-body inelastic channels remains to be seen.

The work carried out in this paper suggests a number of interesting problems, both analytical and numerical, for further investigation.

We have mentioned the problem of including the inelastic channels in the equations, and finding their effect on, for example, the  $\rho$  width.

A critical test of our equations can come from a determination of the fermion trajectories, using the equations derived in Sec. II. For example, if we supply the mass of the nucleon and the  $\pi NN$  coupling strength, can we predict the position and width of the  $f_3$  resonance that is believed to lie on the nucleon trajectory? If so, the same method can be used to discuss all the meson-baryon resonances.

We have noted (Sec. V) that the Pomernchuk trajectory  $\text{Re}\alpha_\rho(t)$  that we obtain is in agreement with that obtained from  $\pi N$  scattering, but not with the results from  $NN$  scattering. This probably means that several Regge poles contribute in an important way to  $NN$  scat-

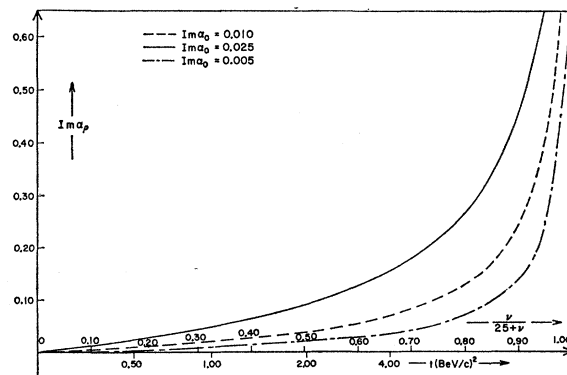


FIG. 15.  $\rho$ -meson trajectory.  $\text{Im}\alpha_\rho(t)$  versus  $t$ ,  $0.08(\text{BeV}/c)^2 < t < \infty$ . The three curves shown were calculated using the input parameters listed in the caption of Fig. 14.

tering at presently explored energies. To achieve a correct understanding of high-energy  $NN$  and  $N\bar{N}$  scattering, which, because of the spin structure of the amplitudes will involve the application of our equations in the many-channel case, forms another interesting and important problem.

Turning now to analytical problems, it is clear that an improvement of the one-pole approximation for the partial-wave amplitude is very desirable. By including the correct contribution of a few nearby poles in the partial-wave amplitude, one could probably obtain satisfactory solutions in *all* instances for the potential case. A representation of the partial-wave amplitudes solely in terms of Regge pole parameters should help such a formulation.

It would be interesting to learn if the zeroes of the residue functions, which appear as input parameters in our equations in their present formulation, can be determined if several poles are coupled together. If this is not the case, how *can* one determine the number and location of the zeroes of a given trajectory? The residue functions of the Pomeranchuk trajectory have a zero when  $\alpha_p$  passes through zero. Since we have not taken account of this fact in the numerical work carried out here, it will be interesting to see how the solutions are modified if a zero is supplied.

Finally, we wish to repeat that one feature of dispersion theory, the crossing symmetry, has so far been totally neglected in our method. An application of the crossing theorem may enable one to determine many of the subtraction constants in a self-consistent manner. Work in this direction is still lacking.

#### ACKNOWLEDGMENTS

The authors wish to thank Professor F. Zachariassen for a number of very stimulating and fruitful discussions.

We are deeply grateful to Dr. G. J. Culler and Dr. B. D. Fried of the Thomson-Ramo-Wooldridge Corporation for their generosity in making available to us the TRW on-line computing system, with the aid of which all the numerical work reported here was carried out. We also wish to thank them for a number of discussions on the numerical aspects of our problem.

It is also a pleasure to thank George Boyd for much assistance in programming and for helpful discussions on the numerical analysis. The aid of Robert Bolman with the computer is also acknowledged.

Finally, we wish to thank Professor S. J. Lindenbaum and Dr. A. Ahmadzadeh, Dr. J. M. Cornwall, Dr. B. J. Kayser, Dr. V. Singh, and Dr. W. G. Wagner for many interesting conversations pertaining to this work.

#### APPENDIX: RELATIONSHIP OF THE TOTAL CROSS SECTION TO THE RESIDUE FUNCTION<sup>27</sup>

The contribution of the Pomeranchuk trajectory to the  $\pi\pi$ -scattering amplitude  $A(s, t)$  is

$$A(s, t) = \frac{1}{3}\beta_p(t) \left\{ \frac{P_{\alpha_p(t)} \left[ - \left( 1 + \frac{2s}{t - 4m_\pi^2} \right) \right] + P_{\alpha_p(t)} \left[ - \left( 1 + \frac{2u}{t - 4m_\pi^2} \right) \right]}{2 \sin \pi \alpha_p(t)} \right\}, \quad (A1)$$

where  $\beta_p(t) = -\pi[2\alpha_p(t) + 1]r_p(t)$ ;  $r_p(t) = \text{Res}A(l, t)_{l=\alpha_p(t)}$ . As  $s, u \rightarrow \infty$ , we have

$$A(s, t) \rightarrow \frac{1}{3} \frac{\beta_p(t) \Gamma(\alpha_p(t) + \frac{1}{2})}{\pi^{1/2} \Gamma(\alpha_p(t) + 1)} \frac{\left[ \left( \frac{e^{-i\pi 4s}}{t - 4m_\pi^2} \right)^{\alpha_p(t)} + \left( \frac{e^{-i\pi 4u}}{t - 4m_\pi^2} \right)^{\alpha_p(t)} \right]}{2 \sin \pi \alpha_p(t)}. \quad (A2)$$

This formula is valid for all  $s$  and  $u$ . Now let us consider the physical region in the  $s$  channel;  $s \rightarrow +\infty$ ,  $t - 4m_\pi^2 < 0$  and fixed. Then  $u = |u|e^{+i\pi}$ . Equation (A2) then gives

$$A(s, t) = \frac{1}{3}\beta_p(t) e^{-i\pi \alpha_p(t)} \frac{\Gamma(\alpha_p(t) + \frac{1}{2})}{\pi^{1/2} \Gamma(\alpha_p(t) + 1)} \left[ \frac{4s}{|t - 4m_\pi^2|} \right]^{\alpha_p(t)} \left[ \frac{e^{-i\pi \alpha_p(t)} + 1}{2 \sin \pi \alpha_p(t)} \right]. \quad (A3)$$

The amplitude  $A(s, t)$  is related to the total  $\pi\pi$ -scattering cross section by

$$\sigma_{\pi\pi}(s) = (16\pi/s) \text{Im}A(s, 0). \quad (A4)$$

Now

$$\text{Im}A(s, t) = \frac{1}{3}\beta_p(t) \frac{\Gamma(\alpha_p(t) + \frac{1}{2})}{\pi^{1/2} \Gamma(\alpha_p(t) + 1)} e^{-i\pi \alpha_p(t)} \left[ \frac{4s}{|t - 4m_\pi^2|} \right]^{\alpha_p(t)} \left( -\frac{1}{2} \right). \quad (A5)$$

Evaluating (A5) at  $t=0$  and setting  $\alpha_p(0)=1$ , we find

$$\begin{aligned} \sigma_{\pi\pi}(\infty) &= (4\pi/3)\beta_p(0) \\ &= -4\pi^2 r_p(0). \end{aligned} \quad (A6)$$

A similar derivation, of course, applies to any other trajectory.

<sup>27</sup> We wish to thank Dr. W. G. Wagner for a helpful discussion of the points covered here.